

Inertial motion tracking of human arm movements in stroke rehabilitation

Huiyu Zhou and Huosheng Hu

Department of Computer Science, University of Essex, Colchester CO4 3SQ, U.K.

E-mail: {zhou,hhu}@essex.ac.uk

Abstract—We present a real-time monitoring system for measuring human upper limb movements in post-stroke rehabilitation. It is based on an advanced inertial sensor MT9 that is commercially available. Human upper limb motion is represented by a kinematic chain in which there are six joint variables to be considered: three for the shoulder and the others for the elbow. Kinematic models are built to study human upper limb motion in three-dimension, based on measurements of the wrist motion. A simulated annealing based optimisation method is adopted to reduce errors in measurements. Experimental results demonstrate the favorable performance of the proposed system in real motion circumstances.

Index Terms—Rehabilitation, tracking, joints, inertial sensor, optimisation.

I. INTRODUCTION

A. Background

Stroke is one of the most important causes of disablement among elderly people. In the UK, around 130,000 people a year suffer a stroke of whom a third end up with severe disability due to the deteriorated motor function in arms and legs. Evidence shows that additional early exercise training may be beneficial [1].

Classical treatments primarily rely on the use of physiotherapy, which depends on the therapists training and past experience. This suggests that traditional methods lack objective standardised analysis for evaluating a patient's performance and assessment of therapy effectiveness [2]. To address this problem, trajectories during the rehabilitation course after stroke have to be quantified, and hence appropriate instruments for the quantitative measurements are desirable to capture motion position and specific details of task execution.

Recently, research has been focused on the issue of measurements of upper limb movements. The state-of-the-art technologies for upper limb motion tracking can be classified as non-vision based, marker-based visual tracking, marker-free visual tracking, and robot assisted systems [3]. Unfortunately, most systems are infeasible in real situations due to computational cost or complicated set-up. Successful examples have existed in literature for the applications of inertial sensor based systems in the measurements of upper limb movements [4]. An inertial sensor can be very small in size and produces fairly accurate linear acceleration (accelerometers) and rate of turn (gyros). However, the

integrated inertial measurements easily suffer from the drift problem.

To seek a reliable estimation for the position or orientation of human movements, one can refer to the numerical algorithms used in solving inverse kinematics problems, consisting of the Newton-Raphson algorithm, differential equation techniques, and optimisation algorithms [5], etc. Unfortunately, these frequently used algorithms can fail due to local minima in the possible solutions. Thus, it is requested that a proper combination of analytical and numerical methods be explored to compensate individual shortcomings.

B. System design

In this paper, we propose an inertial motion tracking system that uses a commercially available inertial sensor MT9 (Xsens Dynamics Technologies, Netherlands). The purpose of the current study is to develop a feasible and reliable system to support a post-stroke rehabilitation program for human upper limbs. The proposed system is computer based, where the inertial sensor MT9 provides tri-axial accelerations and rates of turn, and a software development kit allows 100 Hz sampling rate. The computer is a PC with a Pentium (R) 4/2.8GHz CPU.

The whole system is illustrated in Fig. 1. Using the double buffers on-board, inertial measurements corresponding to human arm movements are consistently generated. Before it can be used for later process, the data has been smoothed in order to maximally reduce noise or instability. The wrist position can be obtained by double integrating the measured accelerations. A kinematic model will exploit this outcome, combining the computed Euler angles, and then provide the position of the elbow joint. Since the positioning of the wrist and elbow is conducted in a sense of integration, the drift problem seems unlikely avoided. Therefore, a Monte Carlo Sampling based optimisation technique, simulated annealing, is adopted in order to attract the estimates near to the true positions in an environment of non-Gaussian errors.

The rest of this paper is arranged as follows. Section II introduces the analytical solution to the kinematic problem of human arm movements. To remedy errors or inconsistency, a fast simulated annealing method is provided in Section III. In Section IV we present a preliminary evaluation on

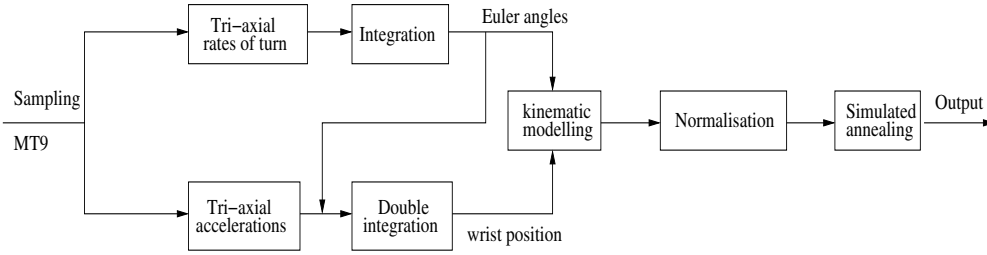


Fig. 1. Structure of the whole system.

the proposed system against a commercial motion tracking system. Finally, this paper is summarised in Section V.

II. KINEMATIC MODELLING

The motion of the human arm could be approximated as an articulated motion of rigid body parts [6]. To simplify the motion estimation, we only take into account a two-joint (shoulder and elbow) upper limb model in this paper. Taking this option enables us to immediately capture the arm motion with a minimum requirement of engaged inertial sensors. However, to respond the request of learning dynamics of a hand, a more complicated upper limb model with the wrist joint will be launched in a future study.

Human arm motions can be represented by kinematic chains. The kinematic chain of our concern consists of six joint variables, i.e. three for the shoulder and the others for the elbow. Note, the proposed system is outstanding from any other existing 7 degree-of-freedom limb model [5], where in the latter the motion of the elbow joint only has one degree-of-freedom. This assumption of one degree-of-freedom is not realistic. For example, it has been discovered that rotation of the forearm (supination/pronation) accompanies regularly repetitive movements, i.e. [7]. To some degree, our system is more reasonable but more challenges are expected, and therefore the motion tracking probably becomes non-trivial. To overcome this impediment, an analytical formulation will be sought to approximately locate the human arm movements. For the purpose of clarification, forward kinematics of the arm motion will be discussed first, followed by an inverse kinematic modelling.

A. Forward kinematics

The forward kinematics specify the Cartesian position and orientation of the local frame attached to the human arm relative to the base frame which is attached to the still joint (shoulder). They are provided by multiplying a series of matrices parameterised by joint angles. Suppose that a kinematic chain is shown in Fig. 2. It is intended to construct the transform that defines frame i to the frame $i-1$, where $i = 1, 2, 3$. In fact, there are two *links* in this particular case, whereas the inertial sensor MT9 is presumably placed upon an area adjacent to the wrist joint.

We begin by defining three intermediate frames for each link - P_1 , P_2 and P_3 . Frame P_3 differs from $i-1$ only by a rotation of β_{i-1} . Frame P_2 has a translation l_{i-1} from P_3 . Frame P_1 differs from P_2 by a rotation θ_i , while frame i differs from P_1 by a translation d_i . Indeed, we can write the transformation that links the pose parameters defined in i to their counterparts in $i-1$ as follows

$${}^{i-1}T_i = {}^{i-1}T_{P_3} T_{P_2}^{P_3} T_{P_1}^{P_2} T_i^{P_1} T \quad (1)$$

This can be generalised as

$${}^{i-1}T_i = \begin{bmatrix} c\theta_i & -s\theta_i & 0 & l_{i-1} \\ s\theta_i c\beta_{i-1} & c\theta_i c\beta_{i-1} & -s\beta_{i-1} & -s\beta_{i-1} d_i \\ s\theta_i s\beta_{i-1} & c\theta_i s\beta_{i-1} & c\beta_{i-1} & c\beta_{i-1} d_i \\ 0 & 0 & 0 & 1 \end{bmatrix} \quad (2)$$

where c and s stand for the cosine and sine functions respectively [8]. The upper arm is connected to the forearm due to the joints and connective tissues. This validates the following expression in the areas, e.g. the shoulder joint,

$$\begin{cases} l_{i-1} = 0 \\ d_i = 0 \end{cases} \quad (3)$$

The point at which the inertial sensor is mounted can be regarded as the end-effector. To simplify the determination of this position, we further assume that the distance between the sensor and the elbow joint has been known *a priori*. The same assumption is also applicable to the distance between the elbow and the shoulder joints.

B. Inverse kinematics

The inverse problem of finding the values of the joint angles given the position of the end-effector is known as the *inverse kinematic problem*. In general, this problem is ill-posed as infinite solutions exist due to the *self-motion manifold*, e.g. a self-motion surface, etc. [9]. With reasonable constraints or prior knowledge, a plausible solution can be found.

Let the coordinates of the elbow and the sensor be denoted by $p_1(x_1, y_1, z_1)$ and $p_2(x_2, y_2, z_2)$, where the latter can be obtained by using the following approximation

$$\mathbf{p}_2(x_2, y_2, z_2)_{i+1} = \mathbf{p}_2(x_2, y_2, z_2)_i + \int_{t_i}^{t_{i+1}} \mathbf{a}_{x_2, y_2, z_2} dt \quad (4)$$

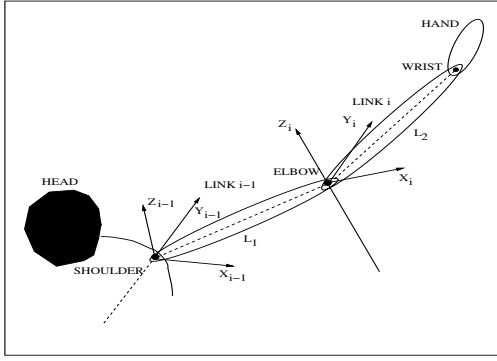


Fig. 2. Kinematics of a two-joint human arm.

where $\mathbf{a}_{x_2, y_2, z_2}$ is the combinatorial acceleration detected by the inertial sensor [10], and t_i and t_{i+1} are two time instants. Assume that L_1 is the distance between the centres of the shoulder and the elbow joints, and L_2 is the distance between the elbow joint and the inertial sensor. Then one can have projected coordinates on three orthogonal planes, i.e. x - y plane

$$\begin{cases} x_2 = \sqrt{L_2^2 - (z_2 - z_1)^2} \cos \phi_z + x_1 \\ y_2 = \sqrt{L_2^2 - (z_2 - z_1)^2} \sin \phi_z + y_1 \end{cases} \quad (5)$$

y - z plane

$$\begin{cases} y_2 = \sqrt{L_2^2 - (x_2 - x_1)^2} \cos \phi_x + y_1 \\ z_2 = \sqrt{L_2^2 - (x_2 - x_1)^2} \sin \phi_x + z_1 \end{cases} \quad (6)$$

x - z plane

$$\begin{cases} x_2 = \sqrt{L_2^2 - (y_2 - y_1)^2} \cos \phi_y + x_1 \\ z_2 = \sqrt{L_2^2 - (y_2 - y_1)^2} \sin \phi_y + z_1 \end{cases} \quad (7)$$

where ϕ_x , ϕ_y and ϕ_z are the Euler angles of the sensor around x -, y - and z -axis, respectively.

Our goal is to estimate the elbow position. This is possible as the inertial sensor allows to acquire angle-related data. Once the elbow position is available, the kinematic parameters corresponding to the links, e.g. orientation and velocity, will be obtained straightforward. However, the solution for the elbow position (x_1, y_1, z_1) is piecewise, which can be segmented as follows:

If $\phi_y = \pm \frac{\pi}{2}$, then

$$x_1 = x_2 \quad (8)$$

When $-\frac{\pi}{2} < \phi_y < \frac{\pi}{2}$, or $\frac{3\pi}{2} < \phi_y < 2\pi$

$$x_1 = x_2 - L_2 \sqrt{\frac{\cos^2(\phi_z) + \sin^2(\phi_x) \sin^2(\phi_z)}{\sin^2(\phi_x) \sin^2(\phi_z) + \frac{1}{\cos^2(\phi_y)}}} \quad (9)$$

Otherwise, if $\frac{\pi}{2} < \phi_y < \frac{3\pi}{2}$, or $-\frac{3\pi}{2} < \phi_y < -\frac{\pi}{2}$

$$x_1 = x_2 + L_2 \sqrt{\frac{\cos^2(\phi_z) + \sin^2(\phi_x) \sin^2(\phi_z)}{\sin^2(\phi_x) \sin^2(\phi_z) + \frac{1}{\cos^2(\phi_y)}}} \quad (10)$$

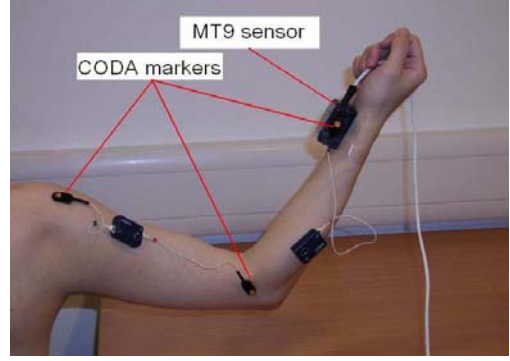


Fig. 3. A human arm attached with a MT9 sensor and three CODA markers.

Eqs. (8), (9) and (10) will not be definite until ϕ_x , ϕ_y , and ϕ_z are entirely determined. The tri-axial gyros in the inertial sensor supply the turning rates, which can be integrated to be angular variations [8]. Substituting Eqs. (8), (9), or (10) to the remainings of Eqs. (5), (6) and (7), the solutions for y and z will be explicitly available, where

$$\begin{cases} y_1 = y_2 - \sqrt{L_2^2 - (x_2 - x_1)^2} \cos(\phi_x) \\ z_1 = z_2 - \sqrt{L_2^2 - (x_2 - x_1)^2} \sin(\phi_x) \end{cases} \quad (11)$$

This technique allows the signs of x_1 , y_1 and z_1 to be correctly determined whilst removing the redundancy of the non-linear system.

x_1 , y_1 and z_1 solely rely on the estimated position of the sensor and the Euler angles. Empirical evidence shows that the acceleration and turning rates usually accompany noise or drifts due to the inherent properties of the inertial sensor. These errors may significantly betray the estimated 3-D positions. One example is shown in Fig. 3. The human arm moves up-to-down repeatedly while the shoulder keeps still. The proposed kinematic modelling based system is compared to a commercially available motion tracking system CODA CX1 (Charnwood Dynamics Ltd, UK) in rendering the elbow position. In this example, three CODA markers are placed around the joints so as to represent them during trajectories. Fig. 4 clearly indicates that there exists unpredictable difference between the outputs of these two systems although they are so close over a period of 7 sec. Spontaneously, we expect an error minimisation to be conducted, which will utilise a simulated annealing technique.

III. SIMULATED ANNEALING

Recall that the distance between the elbow and the shoulder joints has been known as L_1 . Then, we shall have the following *Euclidean distance* constraint (assume that the shoulder joint is the origin of the base frame)

$$x_1^2 + y_1^2 + z_1^2 - L_1^2 = 0 \quad (12)$$

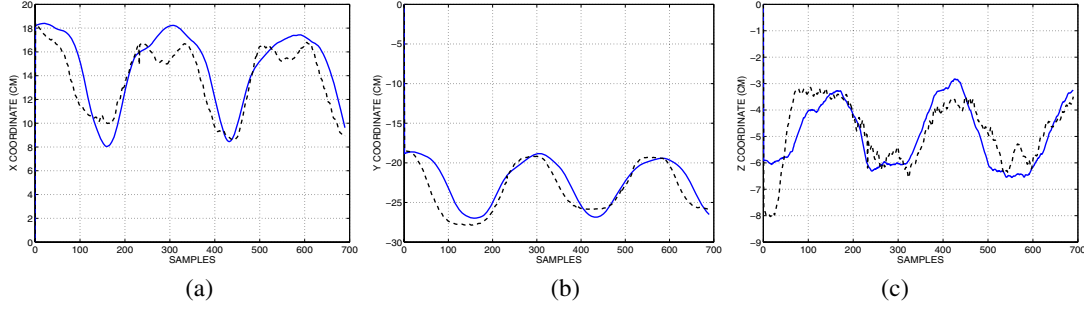


Fig. 4. Estimates of the position of a human elbow joint using the CODA CX1 (solid lines), and the kinematic modelling system (dashed lines).

where x_1 , y_1 , and z_1 are obtained using Eqs. (8), (9), (10) and (11). Irregular over-estimates or underestimates due to noise or erroneous measurements can lead to $|x_1^2 + y_1^2 + z_1^2 - L_1^2| \gg 0$. To enhance the constraint, Eq. (12) can be normalised as

$$\tilde{x}_1^2 + \tilde{y}_1^2 + \tilde{z}_1^2 - L_1^2 = 0 \quad (13)$$

where

$$\begin{cases} \tilde{x}_1 = \frac{x_1 L_1}{\sqrt{x_{11}^2 + y_{11}^2 + z_{11}^2}} \\ \tilde{y}_1 = \frac{y_1 L_1}{\sqrt{x_{11}^2 + y_{11}^2 + z_{11}^2}} \\ \tilde{z}_1 = \frac{z_1 L_1}{\sqrt{x_{11}^2 + y_{11}^2 + z_{11}^2}} \end{cases} \quad (14)$$

where (x_{11}, y_{11}, z_{11}) are the coordinates of the first sample in the sequence. Indeed, a generic generalised format for Eq. (13) is yielded as follows

$$E(\tilde{x}_1, \tilde{y}_1, \tilde{z}_1) \propto \arg \min(\tilde{x}_1^2 + \tilde{y}_1^2 + \tilde{z}_1^2 - L_1^2) \quad (15)$$

To pursue a global solution to the minimisation problem as Eq. 15, the method of simulated annealing is applied with the given set of measurements and the physical constraint. Simulated annealing is effective and robust in discovering the global optimum. The search of a global minima involves the comparison of the *energies* of two consecutive random conformations. The states at steps $i + 1$ and i are given by v_{i+1} and v_i respectively, where v_i is a six-dimensional vector that includes the tri-axial position of the wrist and the tri-axial angular changes to be optimised. v_{i+1} and v_i are linked together by

$$v_{i+1} = v_i + \Delta v_i \quad (16)$$

where Δv_i is a random perturbation of the six variables. This random perturbation allows v_i to gradually approach to the desired state \tilde{v}_{i+1} . To generate the random vector v_{i+1} one can adopt the *visiting distribution function* $V(\Delta v_{i,j})$ for each component $\Delta v_{i,j}$ of the perturbation vector Δv_i , which is

defined as

$$V(\Delta v_{i,j}) = \left(\frac{q_v - 1}{\pi} \right)^{\frac{1}{2}} \frac{\Gamma\left(\frac{1 - 0.5(q_v - 1)}{q_v - 1}\right)}{\Gamma\left(\frac{1}{q_v - 1} - \frac{1}{2}\right)} \times \frac{(T_{q_v}(i))^{\frac{1}{3 - q_v}}}{\left(1 + (q_v - 1) \frac{(\Delta v_{i,j})^2}{(T_{q_v}(i))^{\frac{2}{3 - q_v}}}\right)^{\frac{1}{q_v - 1} - \frac{1}{2}}} \quad (17)$$

where q_v is the visiting index, T_{q_v} is the visiting temperature, and Γ is the gamma function [11].

The vector Δv_i can be obtained by generating random jumps r_i ($0 < r_i < 1$) according to the *visiting distribution function* with the *rejection method*, which is expressed as

$$r_{i+1} = r_i \left(\frac{s_1}{s_r} - s_2 \right) s_c \quad (18)$$

where s_1 and s_2 are two stepping parameters, s_r is a random maximum, and s_c is a scalar.

s_2 and s_c interactively determine the convergence speed and the oscillation amplitude; if either of them is larger, then the solution tends to be more unstable although the final settlement may be more likely to approximate the true solution. Empirically, $s_2 = 0.5$ and $s_c = 0.05$. The energy of the new conformation is compared to the old one, and if this energy is lower than the previous one, the new conformation is then accepted. The comparison is based on the generalised Tsallis probability P_{q_a} [12], and

$$P_{q_a} = \left(1 - \frac{(1 - q_a)(E(v_i) - E(v_{i+1}))}{T_{q_a}(i)} \right)^{\frac{1}{1 - q_a}} \quad (19)$$

where q_a is an acceptance index and $T_{q_a}(i)$ is the acceptance temperature. When $q_a \rightarrow 1$, we are able to recover the Boltzmann-Gibbs statistics used in the classical Metropolis criterion [13].

To guarantee that the final solution gets away from any local minimum, we are supposed to run a large number of iterations. However, this operation will seriously hurt the efficiency of the system, and therefore a real-time mode may not be achieved. As a compromise, we anticipate 30-50 iterations being undertaken that may improve the efficiency

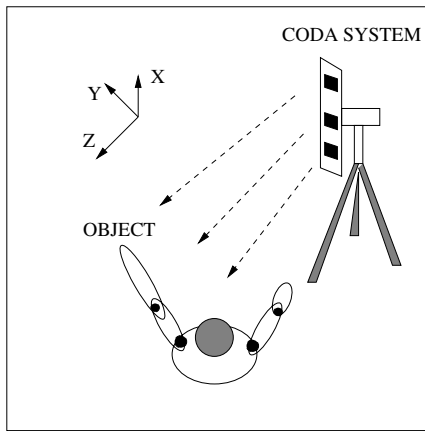


Fig. 5. Experimental set-up in evaluation.

of the optimisation whilst an optimum solution is expected. The solution by using this optimisation strategy will be more accurate as the kinematic modelling system has driven the initial guess closely to the final settlement.

IV. EXPERIMENTAL RESULTS

A. Experimental set-up

In this section, the performance of the proposed kinematic models and the simulated annealing algorithm is in comparison to that of the commercially available motion tracking system CODA CX1. Due to the requirement of real-time operation we are not intending to smooth the estimates for removing spikes and jumps, etc., which is a task beyond the scope of this paper. On the contrary, we are looking at the possibility of maximally reducing the biases so that the final estimation approximates the absolute position supplied from the CODA measurements. Indeed, the goal is to estimate the positions of the wrist and elbow, which are sufficient to be used to describe the movements of the object.

Before the evaluation starts, an experimental environment needs to be set up. Fig. 5 illustrates a subject sitting in front of the CODA system while permitting his left arm moving in a plane perpendicular to the viewing direction of the cameras on the CODA system. The viewing direction of the cameras is aligned with the Z-axis of the world coordinate system, and the X-axis is vertical to the floor. As requested, the MT9 sensor is mounted on an area very close to the wrist joint. In order to avoid relative motion between the marker and the skin (the soft skin effect), a CODA marker is fixated on the MT9 sensor while facing the CODA cameras.

B. Results

The human arm is moved up-to-down repeatedly in the course. We have the measurements of accelerations and Euler angles that look smooth and stable (Fig. 6). After the optimisation by the simulated annealing method, the Euler

angle X significantly shrinks. Other results are omitted due to slight changes. Theoretically, the shrunk angle may lead to the decrease of the travelling distance along the Y- or Z-axis. This assumption is proved in Fig. 7: the deviations in the X coordinates of the wrist and elbow by the simulated annealing are 1.3 and 3.5 cm respectively against approximately 5.6 and 6.5 cm by the kinematic models (Fig. 7 (a) and (d)). Furthermore, it is apparent that some jumps occur in the curve of the optimised Euler angle. This is due to the set-up of s_2 and s_c in Eq. (18): if these values are smaller, then the jumps will be less; otherwise, the jumps will have larger amplitudes. However, the option of smaller s_2 and s_c is dismissed as it will ruin the efficiency of the proposed systems. For the time being, s_2 and s_c stay what they are.

In this test, after adopting the simulated annealing tracking errors have been limited to be less than 3.5 cm in average (Fig. 7 (b) and (c)). This accuracy is much better than that of using kinematic models only, which has an average deviation of 8.4 cm. Similar conclusion can be drawn from Fig. 7 (e) and (f).

V. DISCUSSION AND CONCLUSIONS

In this paper, we have developed kinematic models and simulated annealing algorithms for tracking human arm movements. The justification in experiments has clearly indicated that the proposed simulated annealing scheme is able to achieve a reasonable accuracy, based on the outcomes of the kinematic models. In the experimental results, errors or noise enclosed the outcomes have been found. Since tremors, non-rigid motion or other side-effects often accompany arm movements, this unexpected discrepancy is not surprising. We believe, fundamentally, that if we can encode some filtering techniques, then these errors due to vibration or tremors may be remarkably reduced. In the future work, we also target undertaking a comprehensive testing, which includes a number of pseudo-clinical tasks (for example, reach-mouth tests, and sit-and-stand tests).

ACKNOWLEDGEMENTS

This SMART Rehabilitation Project is supported by the UK EPSRC under Grant GR/S29089/01. The authors would like to thank the Charnwood Dynamics Ltd. that kindly provided the CODA CX1 for the evaluation. The Xsens Dynamics Technologies and the other members of EPSRC EQUAL SMART Rehabilitation Consortium are also acknowledged for valuable discussion.

REFERENCES

- [1] N.F. Gordon, M. Gulanick, F. Costa, G. Fletcher, B.A. Franklin, E.J. Roth, and T. Shephard, "Physical activity and exercise recommendations for stroke survivors," *Circulation*, vol. 109, pp. 2031–2041, 2004.
- [2] R.C.V. Loureiro, C.F. Collin, and W.S. Harwin, "Robot aided therapy: challenges ahead for upper limb stroke rehabilitation," in *The Fifth International Conference on Disability, Virtual Reality and Associated Technologies*, September, 2004.

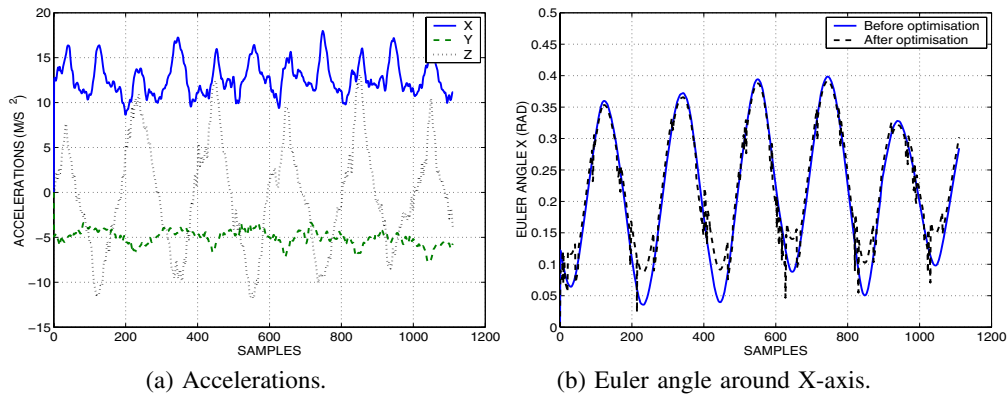


Fig. 6. Acceleration and Euler angle measurements of the MT9 sensor attached at the wrist joint.

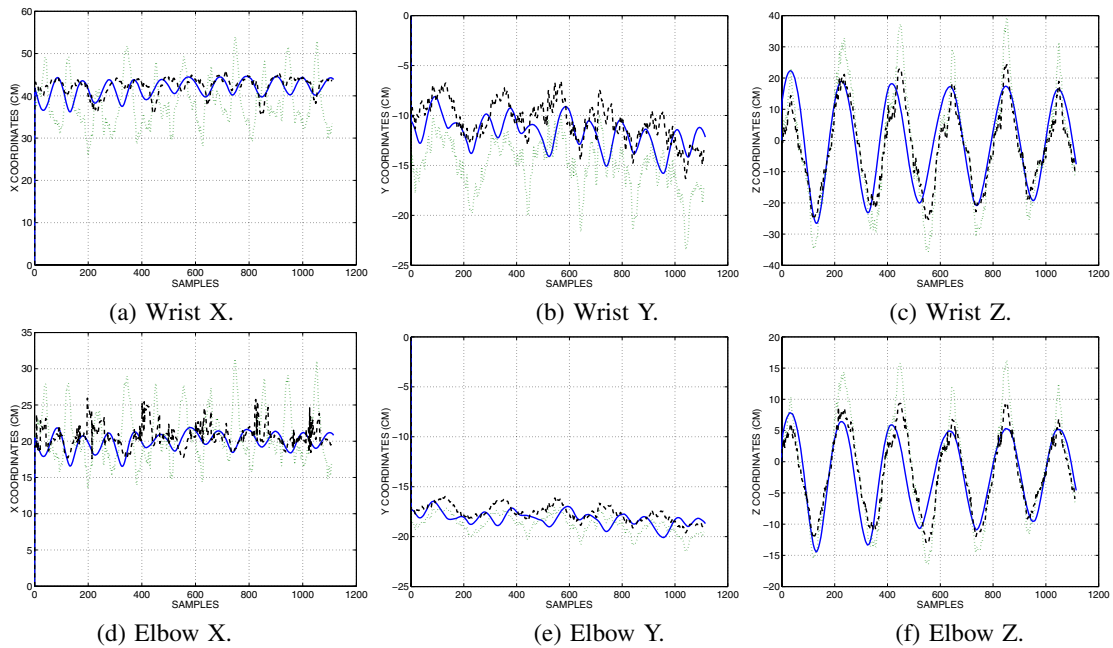


Fig. 7. Measurements of human arm movements (solid lines measured by the CODA system, dotted lines by the proposed kinematic models, and dashed lines by the proposed simulated annealing algorithm based on the outcomes of the kinematic models).

- [3] H Zhou and H. Hu, "A survey - human movement tracking and stroke rehabilitation," Technical Report CSM-420, ISSN 1744 - 8050, University of Essex, UK, 2004.
- [4] V. Krovi, V. Kumar, G.K. Ananthasuresh, and J.M. Vezién, "Design and virtual prototyping of rehabilitation aids," *Journal of Mechanical Design, Transactions of the ASME*, vol. 121, no. 3, pp. 456–458, 1999.
- [5] D. Tolani, A. Goswami, and N.I. Badler, "Real-time inverse kinematics techniques for anthropomorphic limbs," *Graphical Models*, vol. 62, pp. 353–388, 2000.
- [6] A. Ude, "Robust estimation of human body kinematics from video," in *IROS'99*, 1999, pp. 1489–1494.
- [7] M.E. Sesto, R.G. Radwin, W.F. Block, and T.M. Best, "Anatomical and mechanical changes following repetitive eccentric exertions," *Clinical Biomechanics*, vol. 20, pp. 41–49, 2005.
- [8] J.J. Craig, *Introduction to robotics: mechanics and control*, Addison-Wesley, MA, 1989.
- [9] T.B. Moeslund and E. Granum, "Pose estimation of a human arm using kinematic constraints," in *Proc. 12th Scandinavian Conference on Image Analysis*, Jun 11–14, 2001.
- [10] E. Foxlin, Y. Altshuler, L. Naimark, and M. Harrington, "Flighttracker: a novel optical/inertial tracker for cockpit enhanced vision," in *Proc. of ISMAR*, Nov. 2–5, 2004.
- [11] T.J.P. Penna, "Fitting curves by simulated annealing," *Comp. Phys.*, vol. 9, pp. 341–343, 1995.
- [12] C. Tsallis and D. Stariolo, "Generalized simulating annealing," *Phys. A.*, vol. 233, pp. 395–404, 1996.
- [13] N. Metropolis, A.W. Rosenbluth, M.N. Rosenbluth, A.H. Teller, and E.J. Teller, "Equation of state calculation by fast computing machines," *J. Chem. Phys.*, vol. 21, pp. 1087–1092, 1953.